

MODELLING OF WARPING EIGENVIBRATION BY NONUNIFORM TORSION

Justín Murín^{1*}, Mehdi Aminbaghai², Juraj Hrabovský¹, Herbert Mang^{2,3}

¹ Faculty of Electrical Engineering and Information Technology
Slovak University of Technology, Ilkovičova 3, 812 19 Bratislava, Slovakia
justin.murin@stuba.sk, juraj.hrabovsky@stuba.sk

² Institute for Mechanics of Materials and Structures
Vienna University of Technology, Karlsplatz 3, A/1040 Vienna, Austria
mehdi.aminbaghai@tuwien.ac.at, herbert.mang@tuwien.ac.at

³ National RPGE Chair Professor, Tongji University, Siping Road 1239, Shanghai, China,
herbert.mang@tuwien.ac.at

Keywords: Modal Analysis, Nonuniform Torsion, Warping Eigenfrequencies.

Abstract. *This contribution contains a novel investigation of the influence of warping of the cross-section of twisted beams on their eigenvibrations. The investigation is based on the analogy of the bending beam theory and the non-uniform torsion theory of thin-walled open and closed cross-sections. Based on them, the differential equations for dynamic loads, considered as equivalent static loads, are presented. The effect of the secondary torsion moment deformation is taken into account. A part of the first derivative of the twist angle is taken as a warping degree of freedom. The solution of this differential equation is then used for setting up the transfer matrix. The numerical investigation contains the analysis of the natural frequencies and mode shapes of straight cantilever beams with and without consideration of the influence of warping of the cross-section. Beams with open and closed cross-sections are considered. Obtained results are compared with the ones calculated by standard solid and warping beam finite elements.*

1 INTRODUCTION

Beam structures are often exposed to time-dependent loads. Commercial FEM codes allow performing modal and transient dynamic analysis by 3D beam finite elements with and without consideration of the warping effect. Very often the improved Saint-Venant theory of torsion is used and special mass matrices are proposed. Mostly, the bicurvature is chosen as an additional warping degree of freedom and the secondary torsion moment deformation effect (STMDE) is not considered.

For example in [1], the beam element can be used with a lumped or a consistent mass matrix. The consistent mass matrix includes warping effects but does not include the effect of shear deformation. For the standard beam element, the consistent mass matrix is based on reference [2] with the exception that there are additional terms arising from the warping constant I_ω . For the warping element, lumped masses for the warping degree of freedom (bicurvature) are defined [3]. As stated in [1], for solid and closed thin-walled sections, the standard beam element can be used without significant error. However, for the open thin-walled sections, the warping beam element should be used. In [4], the warping beam finite element is recommended to be used only for open thin walled section beams. In [5], the finite beam element is implemented with unrestrained or restrained warping (BEAM188). In [6], the warping beam finite element can be used only for elastostatic analysis of straight beams. It should be noted that in technical practice as well as in the Eurocodes 3 (EC3) the effect of non-uniform torsion by the steel beams with closed cross-sections is not considered.

In the most recent literature relatively little information can be found that refers to the solution for free and forced torsional vibration of beams with hollow cross-sections that include non-uniform torsion effects. In [7], a boundary element method is developed for the nonuniform torsional vibration problem of doubly symmetric composite bars of arbitrary variable cross-section. Dynamic analysis of 3-D beam elements, restrained at their edges, subjected to arbitrarily distributed dynamic loading, is presented in [8]. In [9], Ref. [7] is extended taking the geometrical nonlinearity into account, and in [10], the effect of rotary and warping inertia is implemented. In [11], the nonlinear torsional vibrations of thin-walled beams exhibiting primary and secondary warping are investigated. In [12], a solution for the vibrations of Timoshenko beams by the isogeometric approach is presented, but warping effects are not considered. In [13], geometrically non-linear free and forced vibrations of beams with non-symmetrical cross sections are investigated by the Saint-Venant theory of torsion. In [14], an axial-torsional vibration of rotating pretwisted thin-walled composite box beams, exhibiting primary and secondary warping, are investigated. In [15], a new formulation of a 3D beam element is presented with a new method of describing the transversal deformation of the beam cross-section and its warping.

As follows from the above overview of research papers on the area of nonuniform torsion and of the papers [16], [17], [18], the effect of warping should be considered also by torsion of closed thin-walled section beams. This fact was yet also experimentally proved by elastostatic torsional loading of hollow section beams [17]. It was also shown that the effect of the secondary torsion moment has to be taken into account especially by closed-section beams. Because the bicurvature cannot be used in the constraint equations, e.g. [1], it is straightforward to consider the part of the first derivative of the angle of twist caused by bimoment as the warping degree of freedom also for modal analysis. The new degree of freedom can be used in the constraint condition (it is e.g. exactly equal to zero at the clamped end of the beam), and it can make modal analysis more accurate as this is the case for nonuniform torsion elastostatic analysis [16 – 18]. That is the motivation for the investigation in the following chapters of the present paper.

In chapter 2, the differential equations of 4th order for nonuniform torsion eigenvibrations are established. The part of the bicurvature caused by the bimoment is taken into account as the warping degree of freedom, and the STMDE is also considered. The general semianalytical solution of the differential equation is presented and the transfer matrix relation is established. In chapter 3, the numerical investigation is performed. The results of modal analysis of open I and rectangular hollow cross-section beams by our method are presented and compared with the ones obtained by commercial FEM codes. The effect of STMDE is studied and evaluated. Final assessment of the proposed method and of the obtained results is listed in the summary and conclusions.

2 EIGENVIBRATIONS DUE TO NONUNIFORM TORSION

$$\begin{array}{c} \psi(x) = \psi_M(x) + \psi_S(x) \\ \xrightarrow{x} \quad \xrightarrow{x} \quad \xrightarrow{x} \quad M_\omega(x) \\ M_T(x) = M_{Tp}(x) + M_{Ts}(x) \end{array}$$

Figure 1: Non-uniform torsion: torsional moments and angles of twist.

Fig. 1 refers to determination of the eigenvibrations due to non-uniform torsion. It shows the torsional moment $M_T(x)$, representing the sum of the primary torsional moment $M_{Tp}(x)$ and the secondary torsional moment $M_{Ts}(x)$, and the bimoment $M_\omega(x)$. Fig. 1 also shows the angle of twist, $\psi(x)$, corresponding to $M_{Tp}(x)$. It represents the sum of the angle of twist, resulting from the primary deformation $\psi'_M(x)$ and the secondary deformation $\psi'_S(x)$. Here and in the following, $' := d/dx$.

$$\begin{array}{c} \rho I_\omega \omega^2 \psi'_M(x) \\ \xrightarrow{x} \quad \xrightarrow{x} \\ \rho I_p \omega^2 \psi(x) \\ \xrightarrow{x} \quad \xrightarrow{x} \\ M_\omega(x) \quad M_T(x) \quad M_T(x) + dM_T(x) \quad M_\omega(x) + dM_\omega(x) \\ \xleftarrow{dx} \end{array}$$

Figure 2: Non-uniform torsion: equivalent static line load and line moment acting on an infinitesimal beam element.

Fig. 2 illustrates an infinitesimal element of the beam. It is loaded by the torsional line moment $\rho I_p \omega^2 \psi(x)$ and the line bimoment $\rho I_\omega \omega^2 \psi'_M(x)$, where I_ω stands for the warping constant. These line moments represent the static equivalent of the respective dynamic action. In the following, the equilibrium equations will be formulated, considering the analogy between non-uniform torsion and second-order beam theory, see Table 1. They are obtained as

$$M'_T(x) = -\rho I_p \omega^2 \psi(x), \quad (1)$$

$$M'_\omega(x) = M_T(x) - M_{Tp}(x) + \rho I_\omega \omega^2 \psi'_M(x) = M_{Ts}(x) + \rho I_\omega \omega^2 \psi'_M(x), \quad (2)$$

where

$$M_T(x) = M_{Tp}(x) + M_{Ts}(x). \quad (3)$$

According to Table 1:

$$\psi''_M(x) = -\frac{M_\omega(x)}{EI_\omega}, \quad (4)$$

and

$$\psi'(x) = \psi'_M(x) + \psi'_S(x) \quad (5)$$

with

$$\psi'(x) = \frac{M_{Tp}(x)}{GI_T} \quad (6)$$

$$\psi'_S(x) = \frac{M_{Ts}(x)}{GI_{Ts}}, \quad (7)$$

where I_{Ts} denotes the secondary torsion constant.

Differentiation of equation (5) with respect to x and consideration of the equations (4) and (7) gives

$$\psi''(x) = \psi''_M(x) + \frac{M'_{Ts}(x)}{GI_{Ts}} = -\frac{M_\omega(x)}{EI_\omega} + \frac{M'_{Ts}(x)}{GI_{Ts}}. \quad (8)$$

Making use of the equations (1) and (4) and of the derivative of equation (3) in equation (8) yields

$$\begin{aligned} \psi''(x) &= \psi''_M(x) + \frac{M'_{Ts}(x)}{GI_{Ts}} = -\frac{M_\omega(x)}{EI_\omega} + \frac{M'_T(x) - M'_{Tp}(x)}{GI_{Ts}} = \\ &= -\frac{M_\omega(x)}{EI_\omega} + \frac{-\rho I_p \omega^2 \psi(x) - M'_{Tp}(x)}{GI_{Ts}} = -\frac{M_\omega(x)}{EI_\omega} + \frac{-\rho I_p \omega^2 \psi(x) - GI_T \psi''(x)}{GI_{Ts}}. \end{aligned} \quad (9)$$

Multiplication of equation (9) by EI_ω results in

$$\begin{aligned} EI_\omega \psi''(x) + M_\omega(x) + \frac{EI_\omega}{GI_{Ts}} (\rho I_p \omega^2 \psi(x) + GI_T \psi''(x)) &= \\ = EI_\omega \left(1 + \frac{GI_T}{GI_{Ts}} \right) \psi''(x) + M_\omega(x) + \frac{EI_\omega}{GI_{Ts}} (\rho I_p \omega^2) \psi(x) &= 0. \end{aligned} \quad (10)$$

Differentiation of equation (10) with respect to x and substitution of equation (3) into the so-obtained relation yields

$$EI_\omega \left(1 + \frac{GI_T}{GI_{Ts}} \right) \psi'''(x) + \frac{EI_\omega}{GI_{Ts}} (\rho I_p \omega^2) \psi'(x) + M'_T(x) - M'_{Tp}(x) + \rho I_\omega \omega^2 \psi'_M(x) = 0. \quad (11)$$

Consideration of the equations (5), (6), and (7) in equation (11) yields

$$EI_\omega \left(1 + \frac{GI_T}{GI_{Ts}} \right) \psi'''(x) + \frac{EI_\omega}{GI_{Ts}} (\rho I_p \omega^2) \psi'(x) + M'_T(x) - GI_T \psi'(x) + \rho I_\omega \omega^2 \left(\psi'(x) - \frac{M_{Ts}(x)}{GI_{Ts}} \right) = 0. \quad (12)$$

Differentiation of equation (12) with respect to x and consideration of equation (3) results in

$$EI_\omega \left(1 + \frac{GI_T}{GI_{Ts}} \right) \psi''''(x) + \left(\frac{EI_\omega}{GI_{Ts}} \rho I_p \omega^2 + \rho I_\omega \omega^2 - GI_T \right) \psi''(x) + M'_T(x) - \frac{\rho I_\omega \omega^2}{GI_{Ts}} (M'_T(x) - M'_{Tp}(x)) = 0. \quad (13)$$

Substitution of equation (1) and of the derivative of equation (6) into (13) gives

$$EI_\omega \left(1 + \frac{GI_T}{GI_{Ts}} \right) \psi''''(x) + \left(\frac{EI_\omega}{GI_{Ts}} \rho I_p \omega^2 + \left(1 + \frac{GI_T}{GI_{Ts}} \right) \rho I_\omega \omega^2 - GI_T \right) \psi''(x) + \rho I_p \omega^2 \left(\frac{\rho I_\omega \omega^2}{GI_{Ts}} - 1 \right) \psi(x) = 0. \quad (14)$$

Equation (14) is a linear homogeneous differential equation of fourth order for the angle of twist. It can be verified by means of the analogy between non-uniform torsion and second-order beam theory (see Table 1).

For free-of-warping cross-sections, for which $I_\omega = 0$, equation (14) degenerates to the equation for Saint-Venant torsion.

The general semianalytical solution of the differential equation (14) can be written as follows:

$$\psi(x) = b_0(x)\psi_i + b_1(x)\psi'_i + b_2(x)\psi''_i + b_3(x)\psi'''_i, \quad (15)$$

where $b_0(x)$, $b_1(x)$, $b_2(x)$, $b_3(x)$ denote the transfer functions and ψ_i , ψ'_i , ψ''_i , ψ'''_i represent the integration constants referring to the starting point i (e.g. $\psi_i = \psi_i(x)$ for $x = 0$, etc.).

Equation (15) and its first three derivatives with respect to x are integrated into the following matrix equation:

$$\underbrace{\begin{bmatrix} \psi(x) \\ \psi'(x) \\ \psi''(x) \\ \psi'''(x) \end{bmatrix}}_{\boldsymbol{\psi}(x)} = \underbrace{\begin{bmatrix} b_0(x) & b_1(x) & b_2(x) & b_3(x) \\ b'_0(x) & b'_1(x) & b'_2(x) & b'_3(x) \\ b''_0(x) & b''_1(x) & b''_2(x) & b''_3(x) \\ b'''_0(x) & b'''_1(x) & b'''_2(x) & b'''_3(x) \end{bmatrix}}_{\mathbf{B}(x)} \cdot \underbrace{\begin{bmatrix} \psi_i \\ \psi'_i \\ \psi''_i \\ \psi'''_i \end{bmatrix}}_{\boldsymbol{\psi}_i} \quad (16)$$

In equation (16), $\mathbf{B}(x)$ is a matrix containing the solution functions and its first three derivatives at x , $\boldsymbol{\psi}(x)$ is a vector containing the angle of twist and its first three derivatives at x , and $\boldsymbol{\psi}_i$ is a vector containing the angle of twist and its first three derivatives at the starting point i . The transformation matrix \mathbf{T} in the following matrix equation relates the vector $\boldsymbol{\psi}(x)$ to the “static vector” $\mathbf{Z}(x)$, containing $\psi(x)$, $\psi'_M(x)$, $M_\omega(x)$, and $M_T(x)$.

$$\underbrace{\begin{bmatrix} \psi(x) \\ \psi'_M(x) \\ M_\omega(x) \\ M_T(x) \end{bmatrix}}_{\mathbf{Z}(x)} = \underbrace{\begin{bmatrix} 1 & 0 & 0 & 0 \\ 0 & \left(\frac{\omega^4 EI_\omega \rho I_p \rho I_\omega}{GI_{Ts} (GI_{Ts} - \omega^2 \rho I_\omega)} + \frac{\omega^4 \rho I_\omega^2}{GI_{Ts} - \omega^2 \rho I_\omega} \right) & 0 & \frac{\omega^2 EI_\omega (GI_T + GI_{Ts}) \rho I_\omega}{GI_{Ts} (GI_{Ts} - \omega^2 \rho I_\omega) \left(-\frac{\omega^2 GI_{Ts} \rho I_\omega}{GI_{Ts} - \omega^2 \rho I_\omega} + \frac{\omega^4 \rho I_\omega^2}{GI_{Ts} - \omega^2 \rho I_\omega} \right)} \\ -\frac{EI_\omega}{GI_{Ts}} \rho I_T \omega^2 & 0 & -\frac{EI_\omega (GI_T + GI_{Ts})}{GI_{Ts}} & 0 \\ 0 & \frac{-GI_T GI_{Ts} + \omega^2 (EI_\omega \rho I_p + (GI_{Ts} + GI_T) \rho I_\omega)}{(\rho I_\omega \omega^2 - GI_{Ts})} & 0 & \frac{EI_\omega (GI_T + GI_{Ts})}{\rho I_\omega \omega^2 - GI_{Ts}} \end{bmatrix}}_{\mathbf{T}} \cdot \underbrace{\begin{bmatrix} \psi(x) \\ \psi'(x) \\ \psi''(x) \\ \psi'''(x) \end{bmatrix}}_{\boldsymbol{\psi}(x)} \quad (17)$$

Details concerning determination of \mathbf{T} are given in [20].

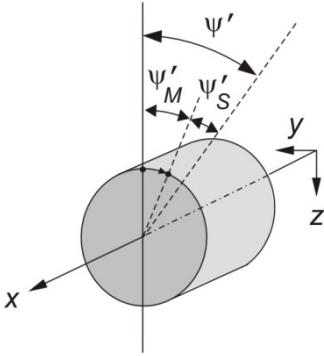
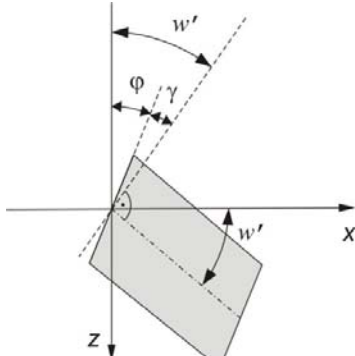
 Non-uniform torsion		 Second-order beam theory	
Angle of twist	$\psi(x)$	$w(x)$	Deflection
Bimoment	$M_\omega(x)$	$M(x)$	Bending moment
Torsional moment	$M_T(x)$	$R(x)$	Transversal force
Primary torsional moment	$M_{Tp}(x)$	$Nw'(x)$	Without a mechanical meaning
Secondary torsional moment	$M_{Ts}(x)$	$V(x)$	Shear force
Derivative of the twist angle with respect to x	$\psi'(x)$	$w'(x)$	Derivative of the deflection with respect to x
Derivative of the twist angle from the primary deformation with respect to x	$\psi'_M(x)$	$\varphi(x)$	Rotation of the cross-section
Derivative of the twist angle from the secondary deformation with respect to x	$\psi'_S(x)$	$\gamma = \frac{V(x)}{GA_s}$	Shear force/Shear stiffness
Torsional stiffness (Saint-Venant)	GI_T	N	Axial force according to second-order beam theory
Secondary torsional stiffness	GI_{Ts}	GA_s	Shear stiffness
Warping stiffness	EI_ω	EI	Bending stiffness
Warping inertia moment	ρI_ω	ρI	Mass inertia moment
Primary torsional inertia moment	ρI_p	ρA	Mass inertia force

Table 1: Analogy between non-uniform torsion and second-order beam theory.

By substitution of equation (16) into (17) the static vector $\mathbf{Z}(x)$ at x is obtained as

$$\mathbf{Z}(x) = \mathbf{F}_{xi}(x) \cdot \mathbf{Z}_i, \quad (18)$$

where \mathbf{Z}_i is the a static vector at the starting point i and $\mathbf{F}_{xi}(x)$ is the transfer matrix, given as

$$\mathbf{F}_{xi}(x) = \mathbf{T} \cdot \mathbf{B}(x) \cdot \mathbf{T}^{-1}. \quad (19)$$

Calculation of the warping eigenfrequencies involves the following steps: At first, the equations (16) and (17) and the transfer matrix $\mathbf{F}_{xi}(x)$ are specialized for the beam length L . The transfer equation (18) is specialized for the nodes i and k to the transfer matrix $\mathbf{F}_{ki}(x=L)$. Taking into account the boundary conditions, the reduced system of two homogeneous algebraic equations is obtained. The circular natural frequencies ω_j , $j = 1, 2, \dots$, follow from

the zeros of the determinant of the reduced system of equations. An iterative method was used to find the zeros of the determinant. The natural frequencies $f_j = \omega_j / 2\pi$, $j = 1, 2, \dots$, are determined subsequently.

The above algorithm was implemented into the software MATHEMATICA [21]. The eigenfrequencies were calculated for cantilever beams with thin-walled open and closed cross-sections. In chapter 3, the results of the numerical experiments are presented and compared with the results obtained from the available commercial software.

3 NUMERICAL EXAMPLES

In this chapter, the results of modal analysis concerning the nonuniform torsion eigenmodes of chosen open and closed shaped beams are investigated.

3.1 Cantilever beam with an I cross-section

Saint-Venant and nonuniform torsion eigenfrequencies of the cantilever beam (Fig. 3) with length $L = 2$ m were calculated. The cross-section is the one of a HEA-100 [22]. In Table 2 and Table 3, the cross-sectional parameters and the material properties are listed, respectively.

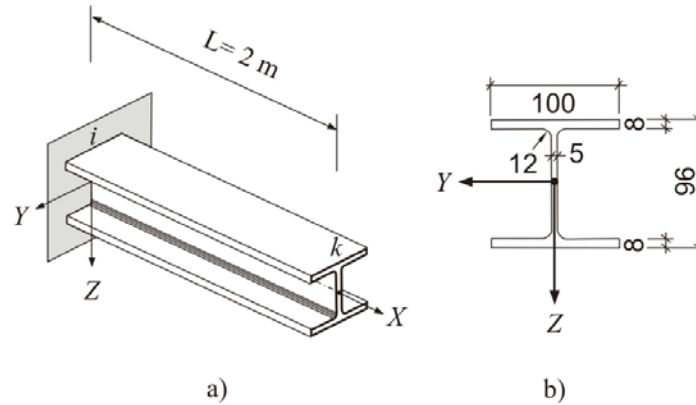


Figure 3: Cantilever beam with an I cross-section a) system, b) cross-section.

Cross-sectional parameters [22]:		
Polar moment of inertia:	$I_p = I_y + I_z = 4830 \cdot 10^{-9}$	m^4
Torsion constant:	$I_T = 52.4 \cdot 10^{-9}$	m^4
Secondary torsion constant:	$I_{Ts} = 2581.3 \cdot 10^{-9}$	m^4
Warping constant:	$I_\omega = 258.1 \cdot 10^{-11}$	m^6

Table 2: Cross-sectional parameters for nonuniform torsion.

Material characteristics:		
Young's modulus:	$E = 21 \cdot 10^7$	kN/m^2
Poisson's ratio:	$\nu = 0.3$	
Shear modulus:	$G = 8.0769 \cdot 10^7$	kN/m^2
Mass density:	$\rho = 7.85$	t/m^3

Table 3: Material properties.

In the torsional modal analysis the following boundary conditions were applied:

a) Saint-Venant torsional vibration:

$$\psi(x)|_{x=0} = \psi_i = 0, \quad M_T(x)|_{x=L} = M_{T,k} = 0. \quad (20)$$

d) Warping vibration (according to chapter 2):

$$\begin{aligned} \psi(x)|_{x=0} = \psi_i = 0, \quad \psi'_M(x)|_{x=0} = \psi'_{M,i} = 0, \\ M_\omega(x)|_{x=L} = M_{\omega,k} = 0, \quad M_T(x)|_{x=L} = M_{T,k} = 0. \end{aligned}$$

Important notice: According to the analogy between non-uniform torsion and second-order beam theory (Table 1), it holds at the clamped beam end:

for the flexural vibration case $\frac{\partial w}{\partial x}|_{x=0} = w'_i \neq 0$ but $\varphi|_{x=0} = \varphi_i = 0$; and for the warping

vibration $\frac{\partial \psi}{\partial x}|_{x=0} = \psi'_i \neq 0$ but $\frac{\partial \psi'_M}{\partial x}|_{x=0} = \psi'_{M,i} = 0$.

Table 4 contains a comparison of the results for the first three eigenfrequencies with corresponding results obtained by the computer programs RSTAB [6] and ANSYS [5]. All values were obtained by the mentioned computers programs with following number of finite elements:

- 39700 elements of the type SOLID186 and 200 elements of the type BEAM188 – ANSYS [5];
- 50 elements of the type BEAM – RSTAB [6].

Type of eigenvibrations	Eigenfrequencies [Hz]			
	f_j	Proposed method	RSTAB [6]	ANSYS [5] SOLID186/BEAM188
Saint-Venant torsion about the x -axis	f_1	41.7	41.7	---/36.3
	f_2	125.2	125.5	---/109.1
	f_3	208.8	209.9	---/181.9
Warping torsion about the x -axis including deformations due to the secondary torsional moment	f_1	51.4	-----	50.8/---
	f_2	177.4	-----	172.8/---
	f_3	366.2	-----	356.8/---
Warping torsion about the x -axis without deformations due to the secondary torsional moment	f_1	51.6	-----	50.8/46.5
	f_2	178.7	-----	172.8/165.5
	f_3	373.0	-----	356.8/356.7

Table 4: First three eigenfrequencies of a cantilever beam with an I cross-section.

As expected, the difference between the uniform torsional eigenfrequencies (Saint-Venant) and the eigenfrequencies obtained by the proposed method and the commercial programs RSTAB [6] are negligible. But there is a visible deviation from the BEAM188 (warping unrestrained) results. These discrepancies are caused by the fact that in the FEM model based

on BEAM188 element the non-round transition between the web and the flange of I - profile was assumed, which has a small influence on the cross-sectional characteristics.

In nonuniform torsion analysis without STDME by the proposed approach and by the BEAM188 finite element with restrained warping the eigenfrequencies difference has decreased. The both results agree relatively well also with the SOLID186 solution results.

Our nonuniform torsion approaches with and without STMDE produce nearly the same results, what proves the fact, that the secondary torsion moment does not play significant role in torsion of open-section beams. On the other hand, the first three eigenfrequencies calculated with STMDE are closer to the SOLID186 solution results.

The first three torsional modes of the beam are shown in Fig. 4 and 5. They were obtained by means of the SOLID186 finite element [5]. It is seen that the cross-section satisfies the deformation conditions for nonuniform torsion of thin-walled cross-sections, as given by the thin tube theory (TTT). The torsional eigenmodes can be evaluated by means of the transfer relations (17), but the graphical representation is quite cumbersome (as it is also the case for the beam finite elements). This problem will be treated in our future work.

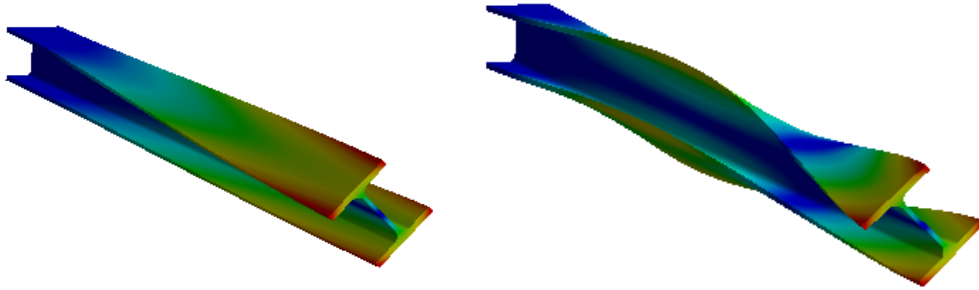


Figure 4: Mode shapes corresponding to the first and the second warping eigenfrequencies [5].

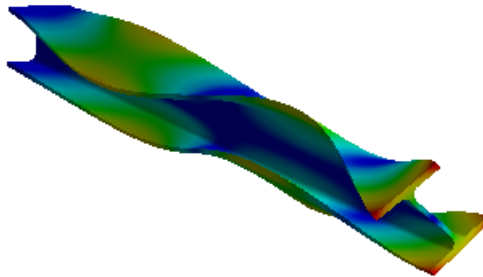


Figure 5: Mode shape corresponding to the third warping eigenfrequency [5].

3.2 Warping eigenfrequencies and mode shapes of a cantilever rectangular hollow section beam with constant ratio of $h/b = 80/40$ and $h/b = 50/40$, and with variable length L and wall thickness t .

Fig. 6 refers to the investigated cantilever beam. Fig. 6(a) shows the rectangular hollow beam and Fig. 6(b) illustrates the cross-section.

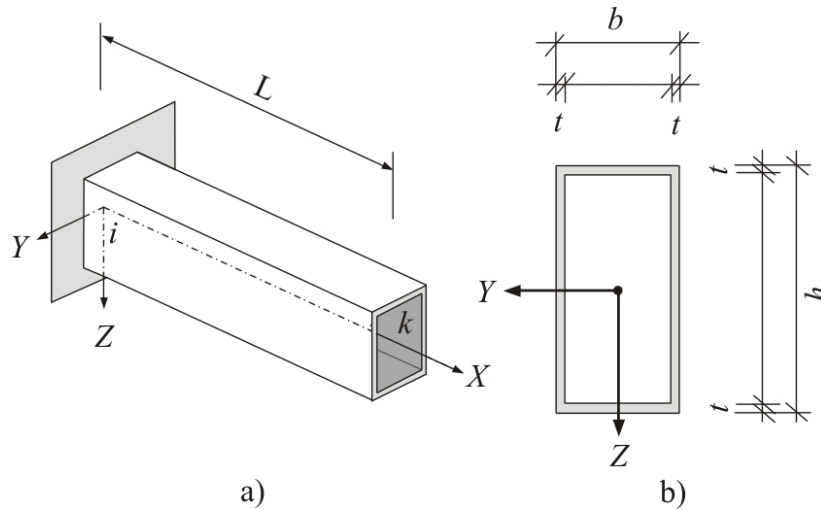


Figure 6: Cantilever beam with a rectangular hollow cross-section: a) system, b) cross-section.

The chosen material characteristics and the cross-sectional parameters are listed in Tables 3 and 5. The boundary conditions are the same as in section 3.1, expressions (20) and (21). In the following, the cross-sectional parameters and the cross-sectional characteristics are calculated by ANSYS [4] and [23] for $t = 5$ mm and $t = 10$ mm:

Cross-sectional parameters [5], [23] :			
Cross-sectional area [5]:	$h/b/t = 40/40/5$	$A = 7 \cdot 10^{-4}$	m^2
	$h/b/t = 40/40/10$	$A = 12 \cdot 10^{-4}$	
	$h/b/t = 50/40/5$	$A = 8 \cdot 10^{-4}$	
	$h/b/t = 50/40/10$	$A = 14 \cdot 10^{-4}$	
	$h/b/t = 60/40/5$	$A = 9 \cdot 10^{-4}$	
	$h/b/t = 60/40/10$	$A = 16 \cdot 10^{-4}$	
	$h/b/t = 70/40/5$	$A = 10 \cdot 10^{-4}$	
	$h/b/t = 70/40/10$	$A = 18 \cdot 10^{-4}$	
	$h/b/t = 80/40/5$	$A = 11 \cdot 10^{-4}$	
	$h/b/t = 80/40/10$	$A = 20 \cdot 10^{-4}$	

Polar moment of inertia [5, 23]:	$h/b/t = 40/40/5$ $h/b/t = 40/40/10$	$I_p = I_y + I_z = 29.167 \cdot 10^{-8}$ $I_p = I_y + I_z = 40.000 \cdot 10^{-8}$	m^4
	$h/b/t = 50/40/5$ $h/b/t = 50/40/10$	$I_p = I_y + I_z = 43.333 \cdot 10^{-8}$ $I_p = I_y + I_z = 61.833 \cdot 10^{-8}$	
	$h/b/t = 60/40/5$ $h/b/t = 60/40/10$	$I_p = I_y + I_z = 61.500 \cdot 10^{-8}$ $I_p = I_y + I_z = 90.667 \cdot 10^{-8}$	
	$h/b/t = 70/40/5$ $h/b/t = 70/40/10$	$I_p = I_y + I_z = 84.167 \cdot 10^{-8}$ $I_p = I_y + I_z = 127.500 \cdot 10^{-8}$	
	$h/b/t = 80/40/5$ $h/b/t = 80/40/10$	$I_p = I_y + I_z = 111.833 \cdot 10^{-8}$ $I_p = I_y + I_z = 173.333 \cdot 10^{-8}$	
Torsion constant [5]:	$h/b/t = 40/40/5$ $h/b/t = 40/40/10$	$I_T = 23.111 \cdot 10^{-8}$ $I_T = 33.068 \cdot 10^{-8}$	m^4
	$h/b/t = 50/40/5$ $h/b/t = 50/40/10$	$I_T = 33.099 \cdot 10^{-8}$ $I_T = 48.812 \cdot 10^{-8}$	
	$h/b/t = 60/40/5$ $h/b/t = 60/40/10$	$I_T = 43.641 \cdot 10^{-8}$ $I_T = 65.382 \cdot 10^{-8}$	
	$h/b/t = 70/40/5$ $h/b/t = 70/40/10$	$I_T = 54.561 \cdot 10^{-8}$ $I_T = 82.473 \cdot 10^{-8}$	
	$h/b/t = 80/40/5$ $h/b/t = 80/40/10$	$I_T = 65.753 \cdot 10^{-8}$ $I_T = 99.913 \cdot 10^{-8}$	
Secondary torsion constant [23]:	$h/b/t = 40/40/5$ $h/b/t = 40/40/10$	$I_{Ts} = 0.169 \cdot 10^{-8}$ $I_{Ts} = 9.836 \cdot 10^{-9}$	m^4
	$h/b/t = 50/40/5$ $h/b/t = 50/40/10$	$I_{Ts} = 0.374 \cdot 10^{-8}$ $I_{Ts} = 8.040 \cdot 10^{-9}$	
	$h/b/t = 60/40/5$ $h/b/t = 60/40/10$	$I_{Ts} = 2.048 \cdot 10^{-8}$ $I_{Ts} = 28.418 \cdot 10^{-9}$	
	$h/b/t = 70/40/5$ $h/b/t = 70/40/10$	$I_{Ts} = 4.503 \cdot 10^{-8}$ $I_{Ts} = 62.903 \cdot 10^{-9}$	
	$h/b/t = 80/40/5$ $h/b/t = 80/40/10$	$I_{Ts} = 7.910 \cdot 10^{-8}$ $I_{Ts} = 12.754 \cdot 10^{-8}$	

Warping constant [5]:	$h/b/t = 40/40/5$ $h/b/t = 40/40/10$	$I_{\omega} = 0.160 \cdot 10^{-12}$ $I_{\omega} = 46.796 \cdot 10^{-14}$	m^6
	$h/b/t = 50/40/5$ $h/b/t = 50/40/10$	$I_{\omega} = 1.080 \cdot 10^{-12}$ $I_{\omega} = 23.901 \cdot 10^{-13}$	
	$h/b/t = 60/40/5$ $h/b/t = 60/40/10$	$I_{\omega} = 4.652 \cdot 10^{-12}$ $I_{\omega} = 92.648 \cdot 10^{-13}$	
	$h/b/t = 70/40/5$ $h/b/t = 70/40/10$	$I_{\omega} = 12.371 \cdot 10^{-12}$ $I_{\omega} = 23.610 \cdot 10^{-12}$	
	$h/b/t = 80/40/5$ $h/b/t = 80/40/10$	$I_{\omega} = 25.762 \cdot 10^{-12}$ $I_{\omega} = 47.890 \cdot 10^{-12}$	

 Table 5: Cross-sectional parameters [4] and [23] for $t = 5$ and 10 mm.

The aim of the investigation is the evaluation of the influence of the warping and the STMDE on the eigenfrequencies of the closed-section beam depending on the beam length and the wall thickness.

Tables 6 – 8 contains a comparison of the results for the first three torsional eigenfrequencies obtained by proposed method (Saint-Venant torsion, in lines a) and non-uniform torsion with STMDE, in lines b)) and with corresponding results obtained by the computer programs RSTAB [6] and ANSYS [5] for $t = 5$ mm and $t = 10$ mm, respectively. The results of RSTAB [6] are based on number of 50 Saint-Venant torsion beam finite elements (denoted by WW-E). The results of ANSYS [5] solution are based on number of 37 500 of SOLID186 elements (denoted by 3D-E) and on number of 100 of BEAM188 elements (warping unrestrained) denoted by WW-E, and non-uniform torsion (warping restrained without STMDE) denoted by W-E.

	Type of eigen-vibrations	Eigenfrequencies [Hz]				
		f_j	Proposed method	Type of elements	RSTAB [6]	ANSYS [5]
$h/b/t = 80/40/5$ $L = 100$ [mm]	a)	f_1	6149.0	WW-E	6149.0	6149.0
		f_2	18446.8	WW-E	18447.3	18449.0
		f_3	30744.7	WW-E	30746.8	30753.0
	b)	f_1	6333.0	W-E	-----	6205.8
				3D-E	-----	7493.8
		f_2	19017.8	W-E	-----	19827.0
				3D-E	-----	22315.0*
		f_3	30530.2	W-E	-----	36090.0
$h/b/t = 80/40/5$ $L = 200$ [mm]	a)	f_1	3074.5	WW-E	3074.5	3074.5
		f_2	9223.4	WW-E	9223.5	9224.3
		f_3	15372.4	WW-E	15372.6	15376.0
	b)	f_1	3126.9	W-E	-----	3082.9
				3D-E	-----	4041.8
		f_2	9417.1	W-E	-----	9442.7
				3D-E	-----	10957.0*
		f_3	15825.5	W-E	-----	16322.0
				3D-E	-----	18816.0*

$h/b/t = 80/40/5$ $L = 300$ [mm]	a)	f_1	2049.6	WW-E	2049.6	2049.7
		f_2	6148.9	WW-E	6148.9	6149.5
		f_3	10248.2	WW-E	10248.3	10251.0
	b)	f_1	2073.3	W-E	-----	2052.3
				3D-E	-----	3306.8
		f_2	6240.9	W-E	-----	6218.9
				3D-E	-----	7497.3*
		f_3	10463.0	W-E	-----	10562.0
				3D-E	-----	11961.0*
$h/b/t = 80/40/5$ $L = 400$ [mm]	a)	f_1	1537.2	WW-E	1537.2	1537.3
		f_2	4611.7	WW-E	4611.7	4612.1
		f_3	7686.2	WW-E	7686.2	7688.2
	b)	f_1	1550.5	W-E	-----	1538.4
				3D-E	-----	1430.8
		f_2	4663.4	W-E	-----	4642.3
				3D-E	-----	5728.0*
		f_3	7807.2	W-E	-----	7825.3
				3D-E	-----	9221.4*
$h/b/t = 80/40/5$ $L = 500$ [mm]	a)	f_1	1229.8	WW-E	1229.8	1229.8
		f_2	3689.4	WW-E	3689.4	3689.7
		f_3	6149.0	WW-E	6149.0	6150.5
	b)	f_1	1238.2	W-E	-----	1230.4
				3D-E	-----	1178.8
		f_2	3721.9	W-E	-----	3705.4
				3D-E	-----	4735.5*
		f_3	6224.5	W-E	-----	6222.5
				3D-E	-----	7464.6*

Table 6: Torsional eigenfrequencies of a cantilever beam with a hollow cross-section (Fig. 6) with $h \times b \times t = 80 \times 40 \times 5$ [mm] and varying length L : a) Saint-Venant torsion; b) Warping torsion including deformations due to the secondary torsion moment.

	Type of eigen-vibrations	Eigenfrequencies [Hz]				
		f_j	Proposed method	Type of elements	RSTAB [7]	ANSYS [4]
$h/b/t = 80/40/10$ $L = 100$ [mm]	a)	f_1	6088.3	WW-E	6088.4	6088.4
		f_2	18265.0	WW-E	18265.4	18267.0
		f_3	30441.7	WW-E	30443.9	30449.0
	b)	f_1	6291.0.1	W-E	-----	6154.7
				3D-E	-----	9096.3*
		f_2	18885.1	W-E	-----	19856.0
				3D-E	-----	22694.0*
		f_3	38296.1	W-E	-----	36482.0
				3D-E	-----	39558.0*

$h/b/t = 80/40/10$ $L = 200$ [mm]	a)	f_1	3044.2	WW-E	3044.2	3044.2
		f_2	9132.5	WW-E	9132.6	9133.3
		f_3	15220.8	WW-E	15221.1	15225.0
	b)	f_1	3102.8	W-E	-----	3054.2
				3D-E	-----	2975.0
		f_2	9346.6	W-E	-----	9392.1
				3D-E	-----	12326.0*
		f_3	15723.6	W-E	-----	16333.0
				3D-E	-----	19293.0*
$h/b/t = 80/40/10$ $L = 300$ [mm]	a)	f_1	2029.4	WW-E	2029.4	2029.5
		f_2	6088.3	WW-E	6088.4	6088.9
		f_3	10147.2	WW-E	10147.3	10150.0
	b)	f_1	2056.1	W-E	-----	2032.6
				3D-E	-----	2019.8
		f_2	6191.5	W-E	-----	6171.8
				3D-E	-----	9200.8*
		f_3	10388.3	W-E	-----	10519.0
				3D-E	-----	13346.0*
$h/b/t = 80/40/10$ $L = 400$ [mm]	a)	f_1	1522.1	WW-E	1522.1	1522.1
		f_2	4566.3	WW-E	4566.3	4566.7
		f_3	7610.4	WW-E	7610.5	7612.4
	b)	f_1	1537.0	W-E	-----	1523.5
				3D-E	-----	1522.0
		f_2	4624.8	W-E	-----	4602.9
				3D-E	-----	8037.7*
		f_3	7747.5	W-E	-----	7776.4
				3D-E	-----	10592.0*
$h/b/t = 80/40/10$ $L = 500$ [mm]	a)	f_1	1217.7	WW-E	1217.7	1217.7
		f_2	3653.0	WW-E	3653.1	3653.3
		f_3	6088.3	WW-E	6088.8	6089.9
	b)	f_1	1227.3	W-E	-----	1218.4
				3D-E	-----	1219.7
		f_2	3689.9	W-E	-----	3672.3
				3D-E	-----	3443.2*
		f_3	6174.5	W-E	-----	6176.2
				3D-E	-----	5061.7*

Table 7: Torsional eigenfrequencies of a cantilever with a rectangular hollow cross-section (Fig. 6) with $h \times b \times t = 80 \times 40 \times 10$ [mm] with varying length L : a) Saint-Venant torsion; b) Warping torsion including deformations due to the secondary torsion moment.

	Type of eigen-vibrations	Eigenfrequencies [Hz]				
		f_j	Proposed method	Type of elements	RSTAB [7]	ANSYS [4]
$h/b/t = 50/40/10$ $L = 100$ [mm]	a)	f_1	7124.9	WW-E	7125.0	7125.0
		f_2	21374.8	WW-E	21375.3	21377.0
		f_3	35624.6	WW-E	35627.1	35634.0
	b)	f_1	7154.1	W-E	-----	7135.1
				3D-E	-----	7145.9
		f_2	21461.6	W-E	-----	21643.0
				3D-E	-----	22261.0*
		f_3	35820.6	W-E	-----	36812.0
				3D-E	-----	36583.0*
$h/b/t = 50/40/10$ $L = 200$ [mm]	a)	f_1	3562.5	WW-E	3562.5	3562.5
		f_2	10687.4	WW-E	10687.5	10688.0
		f_3	17812.3	WW-E	17812.7	17817.0
	b)	f_1	3570.7	W-E	-----	3563.8
				3D-E	-----	3576.3
		f_2	10716.9	W-E	-----	10724.0
				3D-E	-----	10435.0*
		f_3	17880.4	W-E	-----	17980.0
				3D-E	-----	18632.0*
$h/b/t = 50/40/10$ $L = 300$ [mm]	a)	f_1	2375.0	WW-E	2375.0	2375.0
		f_2	7124.9	WW-E	7125.0	7125.6
		f_3	11874.9	WW-E	11875.0	11878.0
	b)	f_1	2378.6	W-E	-----	2375.4
				3D-E	-----	2382.1
		f_2	7138.8	W-E	-----	7136.4
				3D-E	-----	7092.7
		f_3	11906.7	W-E	-----	11928.0
				3D-E	-----	11389.0*
$h/b/t = 50/40/10$ $L = 400$ [mm]	a)	f_1	1781.2	WW-E	1781.2	1781.2
		f_2	5343.7	WW-E	5343.7	5344.2
		f_3	8906.1	WW-E	8906.2	8908.4
	b)	f_1	1783.3	W-E	-----	1781.4
				3D-E	-----	1785.6
		f_2	5351.5	W-E	-----	5348.8
				3D-E	-----	5336.7
		f_3	8923.9	W-E	-----	8929.7
				3D-E	-----	8793.5*
$h/b/t = 50/40/10$ $L = 500$ [mm]	a)	f_1	1425.0	WW-E	1425.0	1425.0
		f_2	4275.0	WW-E	4275.1	4275.3
		f_3	7125.0	WW-E	7125.4	7126.7
	b)	f_1	1426.3	W-E	-----	1425.1
				3D-E	-----	1427.9
		f_2	4279.9	W-E	-----	4277.7
				3D-E	-----	4273.9
		f_3	7136.1	W-E	-----	7137.7
				3D-E	-----	7081.7

Table 8: Torsional eigenfrequencies of a cantilever beam with a hollow cross-section (Fig. 6) with $h \times b \times t = 50 \times 40 \times 10$ mm and with varying length L : a) Saint-Venant torsion; b) Warping torsion including deformations due to the secondary torsion moment.

The main conclusion drawn from Tables 6 – 8 is that, in contrast to the previous example, the influence of warping and the STMDE on the torsional eigenfrequencies of the beam with a rectangular hollow cross-section is not significant. It could be explained by the fact, that the beam stiffness is influenced by warping very locally only. This local action influences strongly the stress state at the restrained cross-sections of the closed sectional beam through the bimoment and secondary torsion moment, but not the eigenfrequency.

As expected, the influence of the STMDE on the eigenfrequency increases with decreasing beam length L . For very small beam length the system is closer to 3D solid. Thus, the beam theory is not longer suitable. For longer beams the warping and the STMDE influence on the torsional eigenfrequencies is less significant.

The best agreement of results obtained by the solid finite elements (denoted by 3D-E) and the proposed method (as well by the Saint-Venant and the warping beam solutions), achieved for the 1st torsional eigenfrequency. For the higher modes the discrepancy increases. The 2nd and 3rd torsional eigenfrequency (denoted as 3D-E and by “*” in Tables 5 – 7) show buckling of the cross-sectional walls. This effect cannot be considered as by the proposed method as by the beam finite elements with restrained and unrestrained warping. These discrepancies are partly reduced by the beam with larger length with smaller section ratio h/b and by greater wall thickness t .

The mode shapes corresponding to the first three torsional eigenfrequencies (obtained by the SOLID186 finite element) are shown in Figs. 7 – 9 (evaluated for $h \times b \times t = 80 \times 40 \times 10$ and $L = 400$ [mm]). Except for the first torsional eigenmode, the cross-section walls are buckling. Therefore a comparison of the eigenfrequencies obtained by means of beam theories with eigenfrequencies based on 3-D solid theory is problematic.

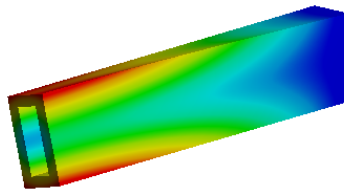


Figure 7: Mode shape corresponding to the 1st torsional eigenfrequency [5].

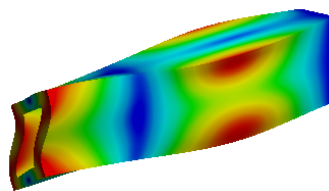


Figure 8: Mode shape corresponding to the 2nd torsional eigenfrequency [5].

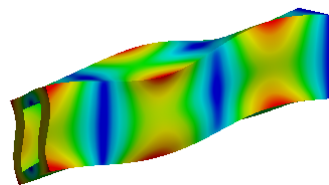


Figure 9: Mode shape corresponding to the 3rd torsional eigenfrequency [5].

4 SUMMARY AND CONCLUSIONS

On the bases of the analogy of the beam theory and the nonuniform torsion theory of thin-walled open and closed cross-sections, the differential equation of 4th order for nonuniform torsion eigenvibration was established. The general semianalytical solution of the differential equation was presented and the transfer matrix relation was established. The results from modal analysis of open I and rectangular hollow section beam by the proposed method were presented and compared with the ones obtained by commercial FEM codes. In the theoretical investigations by the authors, the effect of the secondary torsion moment deformation (STMDE) was taken into account. A part of the first derivative of the twist angle was chosen as a warping degree of freedom. Contrary to the bicurvature, this warping degree of freedom can be used for satisfaction of boundary conditions.

The main conclusions that can be drawn from this investigation are as follows:

(1) Eigenvibrations of open I-section beam:

- The results of modal analysis concerning nonuniform and uniform torsion of open section beams show large differences of the eigenfrequencies. This verifies the well known fact that the warping effect must be taken into account by torsional analysis of open cross-sections in static and in dynamic analysis.
- The proposed approach for calculation of nonuniform torsional eigenvibrations with and without STMDE produces nearly the same results. This proves the fact that the secondary torsion moment does not play a significant role in torsion of open-section beams. On the other side, the torsional eigenfrequencies obtained with STMDE are very close to results obtained by 3D solid finite elements.

(2) Eigenvibrations of rectangular hollow-section beam

- In contrast to the open cross-section, the influence of warping (with or without STMDE) on the nonuniform torsional eigenfrequencies of beams with a rectangular hollow cross-section is not significant. This is explained by the fact, that the beam stiffness is affected by warping only very locally. This has a strong influence on the local stress state at the restrained cross-sections, but not on the eigenfrequency. As expected, the influence of the STMDE on the eigenfrequency increases with decreasing length of the beam. For longer beams the influence of warping and of STMDE on the torsional eigenfrequencies is less significant.
- The best agreement of results obtained by the solid finite elements and the proposed method (as well by the Saint-Venant and the warping beam solutions), achieved for the 1st torsional eigenfrequency. For the higher modes the discrepancy increases. The higher torsional eigenmodes show buckling of the cross-sectional walls. This effect cannot be considered as by the proposed method as by the beam finite elements with restrained and unrestrained warping. These discrepancies are partly reduced by the beam with larger length with smaller section ratio h/b and by greater wall thickness t .
- Because of to the discrepancies between the warping torsion eigenfrequencies of beams with a closed section obtained by the beam theory and the 3D solid theory, an experimental verification of the results is needed.

In future work on the bases of the presented method, a new 3D finite beam element for modal and transient structural analysis will be established, wherein the STMDE and the new warping degree of freedom will be included. It is expected, that for forced torsional vibrations of

closed-section beams, with restrained warping, the effect of warping and of the secondary torsion moment will be stronger than it is in case of modal analysis.

ACKNOWLEDGEMENT

This paper has been supported by the Slovak Grant Agencies APVV-0246-12, VEGA No. 1/0228/14, VEGA No. 1/0453/15 and KEGA No. 007STU-4/2015.

REFERENCES

- [1] ADINA R&D, Inc., *Theory and Modelling Guide. Vol. I: ADINA*. 2013.
- [2] J.S. Przemieniecki, *Theory of matrix structural Analysis*. McGraw-Hill Book Co., 1968.
- [3] K.J. Bathe, A. Chaudhary, On the displacement formulation for torsion of shafts with rectangular cross-section. *Num. Methods in Engineering*, **18**, 1565-1568, 1982.
- [4] ABAQUS/CAE, Version 6.10-1, Dassault Systems Simulia Corp. Providence, RI, USA.
- [5] ANSYS Swanson Analysis System, Inc., 201 Johnson Road, Houston, PA 15342/1300, USA.
- [6] RSTAB, Ingenieur – Software Dlubal GmbH, Tiefenbach 2006.
- [7] E.J. Sapountzakis, Torsional vibration of composite bars of variable cross-section by BEM. *Comp. Meth. Appl. Mech. Engineering*. **194**, 2127-2145, 2005.
- [8] E.J. Sapontzakis, V.G. Mokos, Dynamic analysis of 3-D beam elements including warping and shear deformation effects. *Non-linear Mechanics*. **43**, 6707-6726, 2006.
- [9] E.J. Sapontzakis, V.J. Tsipiras, Nonlinear nonuniform torsional vibration. **329**, 1853-1874, 2010.
- [10] E.J. Sapountzakis, I.C. Dikaros, Non-linear flexural – torsional dynamic analysis of beams of arbitrary cross section by BEM. *Non-linear mechanics*. **46**. 1853-1874, 2011.
- [11] S.A. Sina, H. Haddadpour, Nonlinear free vibration of thin walled beams in torsion.
- [12] S.J. Lee, S.B. Park, Vibrations of Timoschenko beams with isogeometric approach. *Applied mathematical Modelling*. **37**, 9174-9190, 2013.
- [13] S. Stoykov, P. Ribeiro, Non-linear vibrations of beams with non-symmetrical cross sections. *Non-linear Mechanics*. **55**, 153-169, 2013.
- [14] S.A. Sina, H. Haddadpour, Axial – torsional vibrations of rotated pretwisted thin walled composite beams. *Mechanical Sciencies*. **80**, 93-101, 2014.
- [15] K.F. Ferradi, X.A. Cespedes, A new beam element with transversal and warping eigenmodes. *Computers and Structures*. **131**, 12-33, 2014.
- [16] H. Rubin, Wölbkrafttorsion geschlossener Querschnitte und ihrer Irrtümer – Grundlagen. 29. *Stahlbauseminar*. **140**, 2007.
- [17] J. Murín, M. Aminbaghai, V. Kutiš, V. Kralovič, T. Sedlár, V. Goga, H. Mang, A new 3D Timoshenko finite beam element including non-uniform torsion of open and closed cross sections. *Engineering Structures*. **59**, 153 – 160, 2014.

- [18] E.J. Sapountzakis, I.C. Dikaros, Advanced 3D beam element of arbitrary composite cross-section including generalized warping effect. *Numerical Methods in Engineering*. DOI: 10.1002/nme.4849, 2015.
- [19] H. Rubin, Wölbkrafttorsion von Durchlaufträgern mit konstantem Querschnitt unter Berücksichtigung sekundärer Schubverformung. *Stahlbau*. **76**, 826 – 842, 2005.
- [20] M. Aminbaghai, J. Murín, J. Hrabovský, H. Mang, Torsional warping eigenmodes including secondary torsion moment deformation effect. Paper in preparation. 2015.
- [21] Wolfram MATHEMATICA. 9.0.1.0, Wolfran Research, 2013.
- [22] M. Schneider-Bürger, *Stahlbau Profile*. Verlag Stahleisen GmbH, Düsseldorf 2001; Volume 23.
- [23] DUENO, Version 7.01, Dlubal.